Proceedings of the 7th JFPS International
Symposium on Fluid Power, TOYAMA 2008
September 15-18, 2008

P2-12

MEASUREMENT OF FREE AIR IN THE OIL CLOSE TO A HYDRAULIC PUMP

Liselott ERICSON and Jan-Ove PALMBERG

Fluid and Mechanical Engineering Systems
Linkoping University
581 83 Linkoping, Sweden
(E-mail: liselott.ericson@liu.se, jan-ove.palmberg@liu.se)

ABSTRACT

Noise is a well-known challenge in hydraulic systems and hydrostatic pumps are one of the largest noise contributors in a hydraulic system. The existing noise reduction features, such as pressure relief groove and pre-compression filter volume, are more or less dependent on the working condition. It is essential to know the amount of free air when designing a quiet pump; however, it is not evident how much free air the oil contains. The free air content is different if the suction port is boost pressured or self-priming. The amount of free air in a well-designed system can be as low as 0.5% while in others up to 10%.
This paper uses the three-transducer method to measure the amount of free air in the oil. The oil's compressibility can be measured for different working conditions and the free air content can then be calculated. The pre-study is performed with an extensive simulation model. Various noise reduction features' sensitivity to free air content is considered.

KEY WORDS

Air release, noise, flow pulsation, hydraulic pump, measurement

NOMENCLATURE

a :	Wave propagation velocity	[m/s]
E :	Modulus of elasticity	[Pa]
i :	Imaginary unit, $\sqrt{-1}$	[-]
J_0 :	Bessel function of order 0	[-]
J_2 :	Bessel function of order 2	[-]
L :	Length	[m]
N :	Viscous friction factor	[-]
n :	Harmonic number	[-]
P:	Pressure	[Pa]
P_0:	Reference pressure	[Pa]
P_1:	Inlet pressure	[Pa]
P_s:	Discharge pressure	[Pa]
P_v:	Pressure at air measurement device	[Pa]
Q :	Flow	[m^3/s]
r :	Radius	[m]
s :	Laplace operator, $s=i\omega$	[s^{-1}]
T :	Temperature	[°C]
t :	Wall thickness	[m]
x_0 :	Volume fraction of free air at p_0	[-]
x_1 :	Volume fraction of free air at p_1	[-]
Z_C:	Characteristic impedance of the pipe	[Ns/m^5]
Z :	Impedance	[Ns/m^5]
β_e :	Effective bulk modulus	[Pa]
β_f :	Effective fluid bulk modulus	[Pa]
β_{oil}:	Fluid bulk modulus	[Pa]

ρ :	Fluid density	[kg/m^3]
κ :	Polytrophic exponent	[-]
ω :	Frequency	[rad/s]
ν :	Kinematic viscosity	[m^2/s]

Subscripts

i :	Downstream of j	[-]
j :	Upstream of i	[-]

INTRODUCTION

Noise is a well-known challenge in hydraulic systems and hydrostatic pumps are one of the largest noise contributors in a hydraulic system. The existing noise reduction features, such as pressure relief groove and pre-compression filter volume (PCFV), are more or less dependent on the working condition. Rotational speed and pressure variations are the most commonly discussed drive conditions when flow pulsations are considered. Another, less extensively discussed, changing condition is the amount of free air in the oil. The released air from the oil contributes a change in the effective bulk modulus which has an impact on the flow pulsation created in the machine.

A machine works with large pressure differences between the inlet and discharge ports; the fluid properties are therefore not constant. This is principally true of the bulk modulus. In particular, the bulk modulus decreases considerably if the oil contains air bubbles. When the pressure drops below the current saturation pressure level, air is released from the oil and forms air bubbles. The saturation pressure level is not only a fluid parameter but is dependent on the system configuration [1]. Most hydraulic systems are saturated at atmospheric pressure which is at about 1 bar; at this pressure level the oil can dissolve up to 10% volume fraction of air. The air bubbles not only cause a decrease in the bulk modulus, whereby the flow pulsation increases and the efficiency decreases, but also cavitational erosion damage to the surrounding walls when the pressure increases and the released air bubbles collapse. The collapse of the bubbles also causes a broadband spectrum of noise.

The pressure in a hydraulic pump can fall below the saturation pressure level in different ways; when the valve plate is designed with an exaggerated decompression zone or if the inlet kidney closes prematurely, whereby the cylinder tries to suck fluid before it is connected to the inlet port kidney. Another is a result of the jet beam which is created when the valve plate's pre-compression and decompression are insufficient. In this way, substantial high velocity flow pulses are created with and thereby also high dynamic pressure and low static pressure levels. Air bubbles are created and are drawn into the cylinder and have a direct effect on the oil properties at the discharge port.

The third reason for air release in hydraulic pumps is the suction port design. When the inlet port is self-priming, the pressure may decreases when the speed increases and causes a deficiency in fluid in the suction port. Also, when the pressure falls below the saturation pressure level the effective flow decreases due insufficient filling of the cylinders. If the suction port is boost pressurised the insufficient filling problem does not appears.

It is difficult to predict the amount of free air in a pump, since the inlet pressure can differ from one installation to another. The amount of free air in a well-designed system can be as low as 0.5% while in others up to 10%. It is essential to know the amount of free air when designing a quiet pump; however, it is not evident how much free air the oil contains.

This paper considers different noise reduction features' sensitivity to the quantity of free air right at the entrance to the pump. Moreover, the three-microphone method is used to predict the quantity of free air in the suction port.

SIMULATION MODEL

Rotational speed and pressure variations are the most commonly discussed drive conditions when flow pulsations are considered. However, the amount of air released from the oil is significant when designing a quiet machine.

The most common noise reduction features are more or less air content dependent. The features considered in a simulation model are pre- and decompression angles, pressure relief groove [2], and pre-compression filter volume [3].

Simulation techniques are valuable tools in the early stages of the development process. Different simulation models exist for predicting flow ripple in hydrostatic pumps. In this study, a comprehensive simulation model is created in the simulation program HOPSAN, [4] developed at Linkoping University. HOPSAN is used mainly for hydraulic simulations.

The pump model is composed of the number of cylinders in the pump and every cylinder is connected to two orifices. The orifices represent the opening between the suction port and the discharge port and the logic of the opening of these orifices allows simulation of different noise reduction features as pressure relief groove and pre- and decompression angles. Also, additional orifices and volumes can be added to simulate other features like pre-compression filter volume.

The model includes a large number of different states that express the detailed behaviour of the machine. However, the character that is considered in this study is flow pulsation in discharge port.

The fluid properties are not constant during operation. It is chiefly the bulk modulus that varies due to the large pressure differences between discharge and inlet port and also the amount of free air in the oil. In the

simulation model, the free air content is modelled with the tangent value according to Eq. (1).

$$\beta_e = \frac{\beta_{oil}}{1 + \frac{x_0}{\kappa p}\frac{\beta_{oil}}{1-x_0}\left(\frac{p_0}{p}\right)^{\frac{1}{\kappa}}} \quad (1)$$

x_0 is the volume fraction of free air in the oil at reference pressure p_0. β_{oil} is the bulk modulus for oil free from air bubbles. The pressure oscillations can be assumed to be an adiabatic process and at normal hydraulic pressure levels, a realistic polytrophic exponent is about 1.8. The model of the free air content is valid for $x_0 \leq 0.1$.

Simulation results are, however, of little practical use before they are experimentally verified. The comprehensive simulation model has been extensively verified on previous occasions with the two-microphone method [5].

MEASUREMENT OF THE BULK MODULUS

There are different methods of measuring the effective bulk modulus in the high pressure line after the pump; see [6] for a comparison of different methods. The three transducer method is used in this paper and is presented in [7]. The method was used in [8] to test different designs of decompression zones.

The method is based on the pressure waves' propagation in a well defined rigid pipe. The pressure waves are created by the pump in this work. The bulk modulus is calculated indirectly by the measured speed of sound in the measurement pipe.

The point impedance can be calculated at all three transducers along the measurement pipe by using the four pole matrix, see for instance [9]. Equations (2) and (3) show the impedance equations where index *i* is the location upstream of index *j*.

$$Z_i = \frac{P_i}{Q_i} = \frac{Z_c\sqrt{N}\sinh\left(\frac{Ls\sqrt{N}}{a}\right)}{\cosh\left(\frac{Ls\sqrt{N}}{a}\right) - \frac{P_j}{P_i}} \quad (2)$$

$$Z_j = \frac{P_j}{Q_j} = \frac{Z_c\sqrt{N}\sinh\left(\frac{Ls\sqrt{N}}{a}\right)}{\cosh\left(\frac{Ls\sqrt{N}}{a}\right) - \frac{P_i}{P_j}} \quad (3)$$

where

$$Z_c = \frac{\rho a}{\pi r^2} \quad \text{and} \quad N = \frac{J_0\left(ir\sqrt{\frac{s}{\upsilon}}\right)}{J_2\left(ir\sqrt{\frac{s}{\upsilon}}\right)}$$

Using three pressure transducers, index 1-3, separated by lengths L_{12} and L_{23} and with a total length of L_{13}, the point impedance at every transducer can be determined in two ways.

For instance the point impedance at the second transducer can be determined by using Eq. (2) with pressure P_2 (i=2) and pressure P_3 (j=3) and by using Eq. (3) with pressure P_1 (i=1) and P_2 (j=2). In the same way, point impedance at transducer 1 and 3 can be obtained. If the three point impedance is eliminated and the angle-sum relation of the hyperbolic function is used Eq. (4) - (6) are obtained. A clarifying picture of the notation is shown in Figure 1.

$$-\frac{P_3}{P_1}\sinh\left(\frac{L_{12}s\sqrt{N}}{a}\right) + \frac{P_2}{P_1}\sinh\left(\frac{L_{13}s\sqrt{N}}{a}\right) - \sinh\left(\frac{L_{23}s\sqrt{N}}{a}\right) = 0 \quad (4)$$

$$-\frac{P_3}{P_2}\sinh\left(\frac{L_{12}s\sqrt{N}}{a}\right) + \sinh\left(\frac{L_{13}s\sqrt{N}}{a}\right) - \frac{P_1}{P_2}\sinh\left(\frac{L_{23}s\sqrt{N}}{a}\right) = 0 \quad (5)$$

$$-\sinh\left(\frac{L_{12}s\sqrt{N}}{a}\right) + \frac{P_2}{P_3}\sinh\left(\frac{L_{13}s\sqrt{N}}{a}\right) - \frac{P_1}{P_3}\sinh\left(\frac{L_{23}s\sqrt{N}}{a}\right) = 0 \quad (6)$$

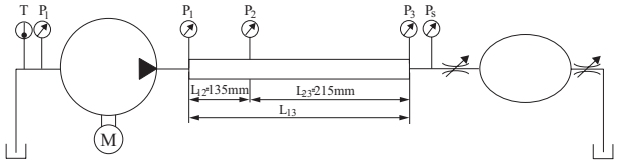

Figure 1 Illustration of the test system.

All three equations ((4)- (6)) are equal and can easily be realised by multiplying Eq (4) with P_1, Eq (5) with P_2, and Eq (6) with P3 which gives Eq. (7).

$$-P_3\sinh\left(\frac{L_{12}s\sqrt{N}}{a}\right) + P_2\sinh\left(\frac{L_{13}s\sqrt{N}}{a}\right) - P_1\sinh\left(\frac{L_{23}s\sqrt{N}}{a}\right) = 0 \quad (7)$$

Only the pump piston harmonics of the pressure spectra are used and therefore Eq. (7) can not be solved exactly to zero. Instead a numerical optimisation algorithm is used to find the wave propagation speed that minimises the left hand side for every harmonic, ε_n. The objective function is formulated as the least square sum according to Eq. (8).

$$F = \sum_1^n \left|\varepsilon_n\right|^2 \quad (8)$$

The complex algorithm [10] is used to solve the minimisation problem of *F*; the algorithm is well suited for the problem and gives fast and repeatable convergence.

Normally, the density can be assumed to be constant and together with the measured wave speed the effective bulk modulus is calculated according to Eq. (9).

$$\beta_e = \rho a^2 \quad (9)$$

The main problem with this technique is considered to be that if not all the frequency spectra of pressure are treated, truncation errors can appear. The measurements carried out in this article are reliable up to about

3000 Hz, which implies that only a few harmonics are considered in high speed measurements. This can be seen as small differences in the speed of sound between different dynamic loads at the same stationary pressure.

CALCULATION OF FREE AIR

The effective bulk modulus includes both the compressibility of the fluid and the wall elasticity. A model for this is considered according to Eq. (10).

$$\beta_e = \frac{1}{\frac{1}{\beta_f} + \frac{r}{2tE}} \tag{10}$$

where β_e is the effective bulk modulus and β_f is the effective fluid bulk modulus. If free air has been released in the oil, the effective fluid bulk modulus is affected and can be modelled as Eq. (11).

$$\beta_f = \frac{\beta_{oil}}{1 + \frac{x_0}{\kappa p}\frac{\beta_{oil}}{1-x_0}\left(\frac{p_0}{p}\right)^{\frac{1}{\kappa}}} \tag{11}$$

x_0 represents the volume fraction of free air at the reference pressure p_0. Equation (11) is actually the same as Eq. (1) considered in the simulation model except that in the measurement the elasticity of the measurement pipe is also considered.

The volume fraction of free air at the pressure level p is determined as

$$x = x_0\left(\frac{p_0}{p}\right)^{\frac{1}{\kappa}} \tag{12}$$

The measurement and calculation of the quantity of released air is approximately due to uncertainties regarding how the air is released from the oil. The air release and the re-saturation take some time and it is not obvious how much of the air is resolved back into the oil during the pressurisation in the machine.

TEST SET-UP

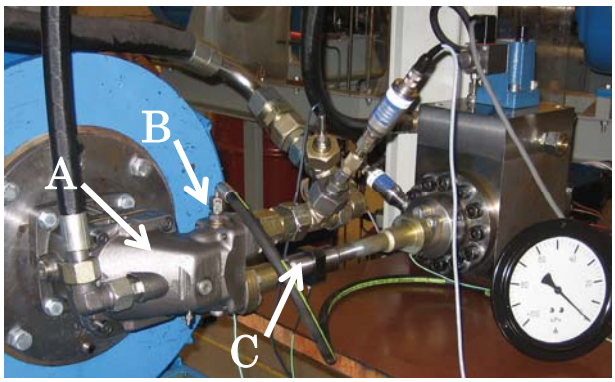

Figure 2 Picture on the test set-up. A is the test pump, B the inlet pressure manometer, and C the measurement pipe with three pressure transducers.

The complete test set-up is shown in Figure 2. The test pump is a 40 cm^3/rev bent-axis piston pump with seven pistons. The tank is located approximately 2 m above the test pump; at very low pump speeds the suction port pressure is therefore about 1.2 bar. The suction port is fairly small and not boost pressured and the pressure is therefore well below atmospheric pressure at higher speeds; see the results section for exact data. The tank volume is about 1 m^3 and the fluid's theoretical circulation time is about 15 minutes at 2000 rpm, which is sufficient to dissolve the air bubbles created anywhere in the circuit.

Three dynamic piezoelectric pressure transducers are located at the measurement pipe to enable measurement of the air content and also the pressure pulsation at the discharge port. The static pressure is measured at the suction port and discharge port. The suction port's manometer is placed right at the pump flange. The pump's inlet channel has equal cross section area from the pump flange to the valve plate and should not give any major differences in the pressure level from the measured pressure to the valve plate. The temperature is measured to maintain a constant temperature throughout the measurements.

RESULTS

The simulation results with different features' sensitivity to free air in the oil are presented first, followed by the measurement results.

Simulation results

The amplitude of the flow pulsations is dependent on the fraction of free are and also the inlet pressure. Figure 3 shows how the amplitude of the discharge flow pulsations alter when the fraction of free air varies from 0 to 5.25 % and Figure 4 how the inlet pressure varies from 0.4 bar up to 10 bar. The discharge flow pulsation is calculated according to Eq. (13).

$$q_{frac} = \frac{q_{\max} - q_{\min}}{q_{mean}} \tag{13}$$

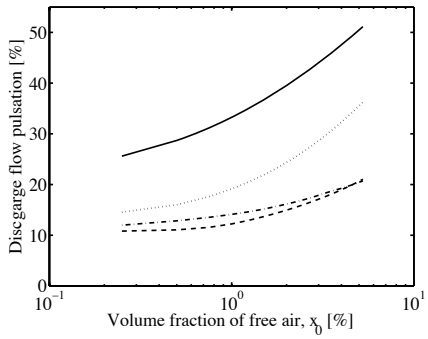

Figure 3 Different noise reduction features' robustness to volume fraction of air, x_0 at inlet pressure 1 bar. The solid line represents simulation for a zero-lapped valve plate, the dotted line pre-compression angle, the dashed line PCFV, and the dashed/dotted line pressure relief groove.

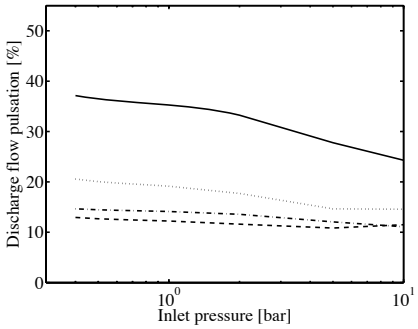

Figure 4 Different noise reduction features' robustness to inlet pressure at x_0=1 %. The solid line represents simulation for a zero-lapped valve plate, the dotted line pre-compression angle, the dashed line PCFV, and the dashed/dotted line pressure relief groove.

The solid line shows a zero-lapped valve plate and as can be seen in Figure 3 an increase in the quantity of free air increases the amplitude of the flow ripple. Boost pressure, Figure 4, also reduces the inlet pressure compared to a self-priming pump.

Figure 3 and Figure 4 show also how robust different common noise reduction features are to variations in air content and inlet pressure in the discharge kidney.

The valve plates with pre-compression filter volume, pressure relief groove, and pre-compression angle are optimised for x_0 = [0, 1, and 5 %] at an inlet pressure of 1 bar. The objective function is the flow pulsation amplitude in the discharge kidney. The pressure is never allowed to fall below 0.3 bar in the optimisation.

The pressure relief groove and pre-compression filter volume is equal sensitive to different volume quantities of free air and inlet pressure. Both pressure relief groove and pre-compression filter volume gives lower amplitude of discharge flow pulsation than pre-compression angle, due the fact that the feature increases the possibilities to avoid cavitation, which is a constraint in the optimisation.

The behaviour of the flow pulsations in the inlet pressure port is the same as for the discharge pressure port.

Measurement results

Speed	p_t [bar]	a [m/s]	β_e [MPa]	x_0 [%]	x_l [%]
900	0.95	1455	1841	1.02	1.05
1100	0.9	1454	1838	1.05	1.11
1200	0.86	1453	1837	1.06	1.16
1400	0.76	1450	1829	1.19	1.36
1500	0.74	1447	1815	1.34	1.59
1600	0.70	1443	1835	1.39	1.69
1700	0.62	1437	1797	1.58	2.06
1800	0.58	1437	1785	1.73	2.33

Table 1 Sound speed measurement with the three-transducer method. The bulk modulus, the fraction of free air at atmospheric pressure, and the suction port pressure are calculated from Eq. (9)-(12).

Measurements of the air content are performed at different rotational speeds at 150 bar and 30°C. Table 1 shows the measurement values when a zero lapped valve plate is used.

The wave propagation velocity, a, is a mean value of two different load cases. The divergence between the load settings measurement is approximately 2 %. However, the results give a reliable trend as can be seen more clearly in Figure 5.

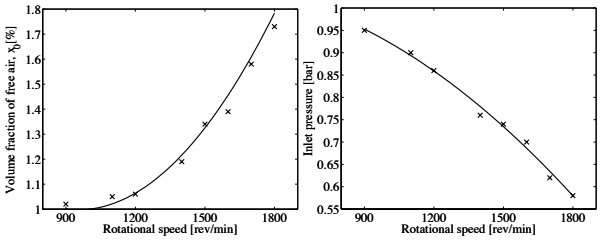

Figure 5 The trend of the volume fraction of released air to the left and inlet pressure to the right when rotational speed increases. Crosses are measurements and solid lines are quadratic equations which are adjusted to the measurements.

The released air increases from 1.02 % to about 1.7 % at atmospheric pressure when the inlet pressure goes from 0.95 bar to 0.58 bar. Provided that no air is created from the inlet port to the measurement pipe the inlet air content can be calculated with Eq. (12) which is shown in very right column of Table 1.

When the pressure varies, the measured fraction of free air also differs. The fraction of free air increases when the pressure increases, as can be seen in Figure 6. The figure shows measurements with two different valve plates. Crosses represent measurements with a zero lapped valve plate and stars a pre-compression angled valve plate. The pre-compression is optimal for a discharge pressure of approximately 60 bar.

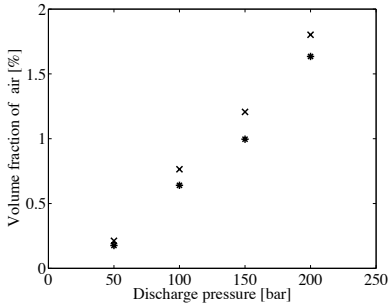

Figure 6 Volume fraction of air at different pressures and valve plate designs. Crosses are with a zero-lapped valve plate while the stars are with a valve plate with pre-compression angle.

DISCUSSION AND CONCLUSION

The simulation results in the paper show some features' robustness to air quantities and inlet pressure.

Implementing a pressure relief groove or a pre-compression filter volume reduces the sensitivity of air content and suction pressure.
The volume fraction of air increases when the speed increases. The main reason for this is probably that the inlet pressure decreases when the speed increases. The filling and emptying speed of the cylinder also increases and the air release can then be delayed which decreases the fraction of air in the oil.
The quantity of released air increases when the discharge pressure increases. The probable cause of this is the jet-beam that is created when the pre-compression is insufficient. The same theory may also be a plausible reason why the pre-compression valve plate creates somewhat less free air than for a zero-lapped valve plate.
All the measurement results show a good picture of the tendency, but the absolute values are less reliable due to uncertainties as regards some parameters.
The paper shows that the valve plate is likely to have an impact on the fraction of free air in the measurement pipe and therefore it is not probable to measure the outlet bulk modulus and predict the fraction of free air in the suction line. The amount of free air should therefore be measured at the inlet to the pump and be compared to the free air content at the discharge port. In this way, the amount of free air created inside the pump can be determined. Further investigation is needed to decide where the air bubbles are created inside the pump, at the discharge port or suction port.

OUTLOOK

Due to the uncertainties as regards the oil properties and the air release behaviour, the results for the quantity of released air are rather approximate. In addition, it is interesting to separate all the air release creating places inside and around the machine. The bulk modulus and thus the volume fraction of air that enters the suction port of the pump should be measured at the suction port. Together with the fraction of free air in the discharge port, the free air created inside the pump can be determined.

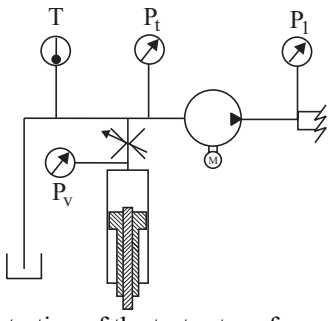

Figure 7 Illustration of the test set-up for measurement of the bulk modulus at the inlet port.

The suction port air content can be measured with a device similar to the piece of equipment used in [11]. A rough illustration of the projected test set-up is shown in Figure 7.

REFERENCES

1. Edge, K.A. and Freitas, F.J.T., A study of pressure fluctuation in the suction lines of positive displacement pumps, Proc. of *the Institution of Mechanical Engineering*, **199**:211-217,1985.
2. Edge, K.A., Designing quieter hydraulic systems - some recent developments and contributions, Proc. of *the Fourth JHPS International Symposium*, Tokyo, Japan, November}, 1999.
3. Pettersson, M., Weddfelt, K., and Palmberg, J-O., Reduction of flow ripple from fluid power piston machines by means of a pre-compression filter volume, Proc. of *Tenth Aachen Colloquium on Fluid Power Technology*, Aachen, Germany, March 17-19, 1992.
4. N.N., *HOPSAN, a simulation package, Users Guide*, Tech Rep. LiTH-IKP-R704, Division of Fluid and Mechanical Engineering Systems, Linkoping University, April, 1998.
5. Weddfelt, K., Measurement of pump source characteristics by the two-microphone method, Proc. of *The Second Tampere International Conference on Fluid Power*, Tampere, Finland, March, 1991.
6. Jinghong, Y. and Kojima, E., Methods for measuring the speed of sound in the fluid transmission pipes, Proc. of *SAE International Off-Highway & Powerplant Congress, Milwaukee*, USA, September, 2000.
7. Johnston, D.N. and Edge, K.A., In-situ measurement of the wavespeed and bulk modulus in hydraulic lines, Proc. of *the Institution of Mechanical Engineering*, **205**:191-197, 1991.
8. Johansson, A. and Palmberg, J-O., The importance of suction port timing in axial piston pumps, *Proc. of The Ninth Scandinavian International Conference on Fluid Power, SICFP'05*, June 1-3, 2005.
9. Viersma, T. J., *Analysis, Synthesis and Design of Hydraulic Servo Systems and Pipelines*, Elsevier scientific publishing company, ISBN 0-444-41869-5, ISSN 0-444-41872-5, 1980.
10. Box, M. J., A New method of constraint optimization and a comparison with other methods, *Computer Journal*, **8**:42-52, 1965
11. Weingarten, F., *Aufbau hydraulischer Zeitglieder und ihr Einsatz im Signalzweig hydraulisch-mechanischer Regelungen*, PhD-thesis, RWTH, Aachen University, Aachen, Germany, 1983